



HEAT AND MASS TRANSFER OF MHD OSCILLATORY VISCOELASTIC FLOW IN A CHANNEL FILLED WITH POROUS MEDIUM

OAHIMIRE, J.I.¹ AND OLAJUWON, B.I.^{2*}

¹Department of Mathematics, Michael Okpara University of Agriculture, Umudike, Nigeria, ²Department of Mathematics, University of Agriculture, Abeokuta, Nigeria

ABSTRACT

Governing equations of heat and mass transfer of MHD oscillatory viscoelastic flow, were formulated, based on assumptions and already existing model. The equations were transformed to dimensionless equations with the aid of non-dimensional variables. Close-form analytical solution was obtained for the dimensionless equations. Graphs were plotted and a table was generated to study the pertinent parameters present in the flow. The result shows that the parameters have significant influences on the flow.

Keywords: Heat transfer, MHD, Mass Transfer, Oscillatory, Porous Medium, Viscoelastic

***Correspondence:** imumolen@yahoo.co.uk, 08063745591

INTRODUCTION

Convective heat transfer is the transfer of heat from one point to another by the movement of fluid. Mass transfer describes the transport of mass from one point to another. Heat and mass transfer is one of the main pillars in the subject of transport phenomenon. It occurs in many processes such as absorption, evaporation, drying, thermal insulation, cooling of nuclear reactor, crude oil extraction, underground energy transport, e.t.c. Oscillating flow means that the fluid motion under consideration possesses a dominant frequency which can be maintained either by an oscillating boundary condition or by an oscillating external force, or by self – oscillations of a flow. Viscoelasticity is the ability of fluid to possess property that exhibit both viscous and elastic characteristics when undergoing deformation. The study of oscillatory viscoelastic fluids through porous media has many scientific and engineering applications. Falade *et al.* [1] investigated the effects of suction/injection on oscillatory flow through a vertical channel with non-uniform wall temperature, the transformed governing equations were solved analytically for analysis. Nandi and Kumbhaker [2] investigated Hall current and thermo-diffusion effects on MHD flow near an oscillatory plate with ramped type thermal and solutal boundary conditions using Laplace transform technique as method of solution.

Olajuwon and Oahimire [3] investigated the effects of Hall current and thermal radiation on heat and mass transfer of unsteady MHD flow of a viscoelastic micropolar fluid through a porous medium using perturbation method. Ali and Asghar [4] studied two – dimensional oscillatory flow inside a rectangular channel for Jeffrey fluid with small suction. The viscoelastic behaviour of non-Newtonian fluids subjected to time harmonic oscillation was investigated with the analytical solution obtained for the governing

equations. Masuda and Tagawa [5] studied quasi-periodic oscillating flows in a channel with suddenly expanded section. Two-dimensional numerical simulation was carried out for an oscillatory flow between parallel flat plates having a suddenly expanded section. The governing equations were discretized and solved numerically for analysis. Tabakova *et al.* [6] considered the oscillatory of Carreau fluid in a channel at different Womersley and Carreau numbers using numerical solution for analysis. Kalpana and Vijaya [7] investigated the effects of suction/injection on unsteady MHD oscillatory second grade fluid flow in a vertical channel with non-uniform wall temperature. Analytical solution was obtained for the dimensionless governing equations w and was used for the analysis of the pertinent parameters present in the flow. Haciogulu and Narayanan [8] investigated effects on species separation by two-dimensional laminar flow arising in a rectangular channel. Saleem *et al.* [9] considered oscillation and radiation effects on MHD Casson fluid model within an asymmetric wavy channel.

The governing equations were handled analytically by choosing the group theoretical method. Sharma and Dubewar [10] investigated the MHD flow between two parallel infinite plate and used finite difference method to obtain solution for analysis. Makinde and Mhone [11] studied heat transfer to MHD oscillatory flow in a channel filled with porous medium. Close-form analytical solution was constructed for the problem which was used for analysis. Choudhury and Das [12] studied the combined effect of a transverse magnetic field and radiative heat transfer on unsteady flow of optically thin viscoelastic fluid through a channel filled with saturated porous medium and non-uniform wall temperature. We extend the work of Choudhury and Das [12] by incorporating concentration equation to investigate heat and mass transfer of MHD oscillatory viscoelastic flow in a channel filled with

porous medium which has not been investigated by any researcher to the best of our knowledge.

Mathematical formulation and method of solution

We consider a conducting optically thin fluid flow in a channel filled with saturated porous medium under the influence of an externally applied magnetic field. The fluid has small electrical conductivity and the electromagnetic force produced is very small. The fluid flow is between two parallel walls at $y' = 0$ and $y' = a$. x-axis is taken along the centre of the channel and y-axis is taken to be perpendicular to it as shown in Figure 1.

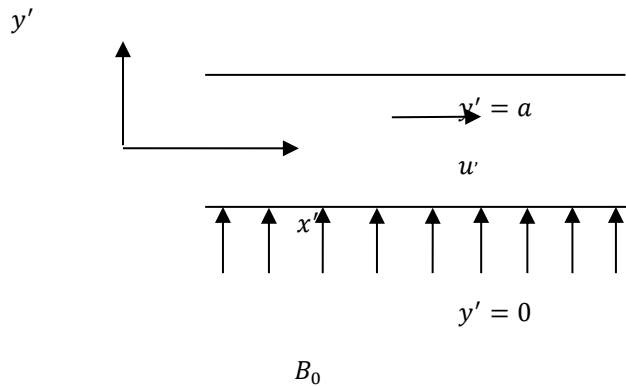


Figure 1: Geometry of the flow.

Assuming Boussinesq incompressible fluid model and extending the work of Choudhury and Das [9], the equations governing the flow in the channel are

$$\frac{\partial u'}{\partial t'} = -\frac{1}{\rho} \frac{\partial p'}{\partial x'} + \nu_1 \frac{\partial^2 u'}{\partial y'^2} + \nu_2 \frac{\partial^3 u'}{\partial y'^2 \partial t'} - \frac{\nu_1}{K} u' - \frac{\sigma B_0^2}{\rho} u' + g\beta_i(T - T_0) + gB_c(C - C_0) \quad (1)$$

$$\frac{\partial T}{\partial t'} = \frac{k}{\rho c_p} \frac{\partial^2 T}{\partial y'^2} - \frac{1}{\rho c_p} \frac{\partial q_r}{\partial y'} \quad (2)$$

$$\frac{\partial C}{\partial t'} = D \frac{\partial^2 C}{\partial y'^2} \quad (3)$$

With the boundary condition given by:

$$u' = 0, T = T_0 + (T_w - T_0)e^{iw't'}, C = C_0 + (C_w - C_0)e^{iw't'} \text{ at } y = a(4)$$

$$u' = 0, T = T_0, C = C_0 \text{ at } y' = 0(5)$$

While u' is the axial velocity, (x', y') is the space coordinates, t' is time, w' is frequency of oscillation, T is the temperature of fluid, C is the mass concentration of the fluid, ρ is the fluid density, p' is the pressure, g is gravitational force, $\nu_i = \mu_i / \rho$ ($i = 1, 2$) is dynamic viscosity, K is the permeability of the porous

medium, $B_0 = (\mu_e, H_0)$ is the electromagnetic induction where μ_e is the magnetic permeability and H_0 is the intensity of magnetic field, σ is the conductivity of the fluid, B_t is the coefficient of volumetric thermal expansion, B_c is the coefficient of volumetric mass expansion, k is the thermal conductivity, C_p is the specific heat at constant pressure, q_r is the radiative heat flux, C_w, C_0, T_w, T_0 and a are concentration at the wall, concentration far from the wall, temperature at the wall, temperature far from the wall and distance between the walls respectively.

Following Cogley *et al.* [13], for optically thin fluid with low density, radiative heat flux is given by:

$$\frac{\partial q_r}{\partial y'} = 4\alpha^2(T_0 - T) \quad (6)$$

where α is the mean radiation absorption coefficient

Then, equation (2) becomes

$$\frac{\partial T}{\partial t'} = \frac{k}{\rho c_p} \frac{\partial^2 T}{\partial y'^2} + \frac{1}{\rho c_p} 4\alpha^2(T_0 - T) \quad (7)$$

We now use the following non-dimensional variables for transformation;

$$y = \frac{y'}{a}, x = \frac{x'}{a}, u = \frac{u'}{U}, t = \frac{t'U}{a}, p = \frac{ap'}{\rho v_1 U}, \theta = \frac{T - T_0}{T_w - T_0}, \phi = \frac{C - C_0}{C_w - C_0}, w = \frac{w'a}{U} \quad (8)$$

Applying equation (8) for transformation, yield the following dimensionless equation.

$$R_e \frac{\partial u}{\partial t} = \frac{-\partial p}{\partial x} + \frac{\partial^2 u}{\partial y^2} + V_0 \frac{\partial^2 T}{\partial y^2 \partial t} - \{S^2 + H^2\}u + Gr\theta + G_c\phi(9)$$

$$P_e \frac{\partial \theta}{\partial t} = \frac{\partial^2 \theta}{\partial y^2} + R^2\theta \quad (10)$$

$$S_c \frac{\partial \phi}{\partial t} = \frac{\partial^2 \phi}{\partial y^2} \quad (11)$$

With the dimensionless boundary conditions:

$$u = 0, \theta = e^{iwt}, \phi = e^{iwt} \text{ at } y = 1(12)$$

$$u = 0, \theta = 0, \phi = 0 \text{ at } y = 0(13)$$

Where $R_e = \frac{Ua}{\nu_1}, V_0 = \frac{\nu_1 U}{\nu_2 a}, S^2 = \frac{1}{Da}, Da = \frac{K}{a^2} H^2 = \frac{\sigma B_0^2 a^2}{\rho \nu_1}, G_r = \frac{g B_t (T_w - T_0) a^2}{\nu_1 U}, G_c = \frac{g \beta_c (T_w - T_0) a^2}{\nu_1 U}$

$p_e = \frac{Ua\rho c_p}{k}$, $R^2 = \frac{4a^2a^2}{\rho v_1}$, $S_c = \frac{Ua}{D}$, are Reynolds number (Re), viscoelastic parameter (Vo), porous medium shape parameter (S), Darcy number (Da), Hartmann number (H), Grashof number (Gr), modified Grashof number (Gc), Peclet number (Pe), radiation parameter (R) and Schmidt (Sc) number respectively.

In order to solve the dimensionless governing equations for purely oscillatory flow, let

$$\frac{\partial P}{\partial x} = Le^{i\omega t} \text{ (where } L \text{ is a constant Nirmala et al. (14))} \quad (14)$$

$$u(y, t) = u_0(y)e^{i\omega t} \quad (15)$$

$$\theta(y, t) = \theta_0(y)e^{i\omega t} \quad (16)$$

$$\phi(y, t) = \phi_0(y)e^{i\omega t} \quad (17)$$

Substituting equation (14) – (17) into (9)-(13), we have:

$$Pu_0''(y) - qu_0(y) = -L - Gr\theta_0(y) - Gc\phi_0(y) \quad (18)$$

$$\theta_0''(y) - r\theta_0(y) = 0 \quad (19)$$

$$\phi_0''(y) - iws_c\phi_0(y) = 0 \quad (20)$$

With the boundary conditions:

$$u_0(y) = 0, \theta_0(y) = 1, \phi_0(y) = 1 \text{ at } y = 1 \quad (21)$$

$$u_0(y) = 0, \theta_0(y) = 0, \phi_0(y) = 0 \text{ at } y = 0 \quad (22)$$

Where $P = (1 + iwV_0)$, $q = iwR_e + \{S^2 + H^2\}$ and $r = R^2 - iwP_e$

Solving (18)-(20) with (21) and (22), yield:

$$u(y, t) = (B_1 e^{n_3 y} + B_2 e^{n_4 y} + B_3 + B_5 \sin(\sqrt{r}y) + B_6 e^{n_1 y} + B_7 e^{n_2 y})e^{i\omega t} \quad (23)$$

$$\theta(y, t) = \frac{\sin(\sqrt{r}y)}{\sin(\sqrt{r})} e^{i\omega t} \quad (24)$$

$$\phi(y, t) = (A_1 e^{n_1 y} + A_2 e^{n_2 y})e^{i\omega t} \quad (25)$$

Where $n_1 = \sqrt{iwSc}$

$$n_2 = -\sqrt{iwSc}$$

$$n_3 = \sqrt{q/p}$$

$$n_4 = -\sqrt{q/p}$$

$$A_1 = \frac{1}{e^{n_1} - e^{n_2}}$$

$$A_2 = -A_1$$

$$B_1 = \frac{(B_3 + B_6 + B_7)e^{n_4} - B_3 - (B_5 \sin(\sqrt{r}) + B_6 e^{n_1} + B_7 e^{n_2})}{e^{n_3} - e^{n_4}}$$

$$B_2 = -(B_1 + B_3 + B_6 + B_7)$$

$$B_3 = \frac{L}{q}$$

$$B_5 = \frac{Gr}{(Pr - q)\sin(\sqrt{r})}$$

$$B_6 = \frac{-GrA_1}{Pn_1^2 - q}$$

$$B_7 = \frac{-GcA_2}{Pn_2^2 - q}$$

The rate of heat and mass transfer across the channel at the upper wall are:

$$N_u = -\frac{\partial \theta}{\partial y} = -\frac{\sqrt{r} \cos(\sqrt{r})}{\sin(\sqrt{r})} e^{i\omega t} \text{ (at } y = 1)$$

$$S_h = -\frac{\partial \phi}{\partial y} = -(n_1 A_1 e^{n_1 y} + n_2 A_2 e^{n_2 y})e^{i\omega t} \text{ (at } y = 1)$$

The rate of heat and mass transfer across the channel at the lower wall are

$$N_u = -\frac{\partial \theta}{\partial y} = -\frac{\sqrt{r}}{\sin(\sqrt{r})} e^{i\omega t} \text{ (at } y = 0)$$

$$S_h = -\frac{\partial \phi}{\partial y} = -(n_1 A_1 + n_2 A_2)e^{i\omega t} \text{ (at } y = 0)$$

RESULTS AND DISCUSSION

Numerical evaluation of the analytical solution of heat and mass transfer of MHD oscillatory viscoelastic flow in a channel filled with porous medium was performed. The results are presented in graphs and in a table. This

was done to know the influences of pertinent parameters in the flow.

TABLE 1: Rate of heat and mass transfer

R	Pe	w	Sc	$-\theta(1)$	$-\theta(0)$
0.5	1.0	1.0	4.0	-0.9000	-1.0344
1.0	1.0	1.0	4.0	-0.6303	-1.1768
1.5	1.0	1.0	4.0	-0.1042	-1.4832
0.5	1.5	1.0	4.0	-0.9121	-1.0174
0.5	2.0	1.0	4.0	-0.9350	-0.9911
0.5	2.5	1.0	4.0	-0.9678	-0.9140
0.5	1.0	1.5	4.0	-0.8808	-0.9321
0.5	1.0	2.0	4.0	-0.8536	-0.8588
0.5	1.0	2.5	4.0	-0.8181	-0.7775
				$-\phi(1)$	$-\phi(0)$
0.5	1.0	1.5	4.0	-1.3328	-0.8983
0.5	1.0	2.0	4.0	-1.4614	-0.8305
0.5	1.0	2.5	4.0	-1.5442	-0.7549
0.5	1.0	1.0	2.0	-1.0153	-0.9525
0.5	1.0	1.0	3.0	-1.0838	-0.8812
0.5	1.0	1.0	4.0	-1.1810	-0.7867

Figure 2 displays the effects of Hartmann number on velocity distribution across the channel. Increase in Hartmann number resulted to decrease in velocity distribution across the channel which is expected because transverse magnetic field gives rise to a resistive type-force called the Lorentz force. This force has the tendency to slow the motion of the fluid. The effects of Reynolds number on velocity distribution across the channel is presented in figure 3. The velocity decreases as Reynolds number increases. Figure 4 depicts the effects of frequency of oscillation on velocity distribution across the layer of the channel. Increase in frequency of oscillation decreases the velocity distribution across the layer of the channel. Figure 5 shows the effects of Peclet number on velocity distribution across the channel and the effect of increase in Peclet number is to increase the velocity of the flow. Figure 6 illustrates the effects of viscoelastic parameter on velocity profiles. The velocity decreases as viscoelastic parameter increases. Figure 7 and figure 8 show the effects of Grashof number and modified Grashof on velocity distribution across the channel respectively. They both increase the velocity distribution across the channel. The effect of radiation parameter is presented in figure 9. As radiation parameter increases, the velocity of the flow also increases. Figure 10 illustrates the effects of Schmidt number on velocity distribution. As can be seen from the

graph, the effect of increase in Schmidt number is to decrease velocity across the channel. Figure 11 shows the effect of porous medium shape parameter on velocity profiles. As the value of porous medium shape parameter increases, the velocity increases. Figure 12 depicts the effects of radiation parameter on temperature profiles. Increase in radiation parameter increases the temperature of the fluid across the channel. The effects of Peclet number on temperature profiles is shown in figure 13. Increase in Peclet number decreases temperature. Figure 14 illustrates the effects of frequency of oscillation on temperature profiles and as frequency of oscillation parameter increases, the temperature decreases. Figure 15 displays the effect of Schmidt number on concentration profiles and it decreases the concentration of the flow. Figure 16 shows the effect of frequency of oscillation parameter on concentration profiles. As can be seen from the figure, it shows that increase in oscillation parameter leads to decrease in concentration.

The effects of radiation parameter, Peclet number, frequency of oscillation parameter and Schmidt number on the rate of heat and mass transfer at both upper and lower wall are shown in the table. Radiation parameter increases the rate of heat transfer at upper wall while it decreases it at the lower wall. Peclet number decreases the rate of heat transfer at upper wall while it increases it at lower wall. As frequency of oscillation increases, rate of heat transfer at both upper and lower wall increases. Schmidt number decreases the rate of mass transfer at upper wall and increases it at lower wall. Frequency of oscillation parameter decreases the rate of mass transfer at upper wall but increases it at lower wall.

CONCLUSION

An analytical study of heat and mass transfer of MHD oscillatory viscoelastic flow in a channel filled with porous medium was conducted. The results are presented and discussed through graphs and a table for pertinent parameters involved. The following conclusion can be drawn from the result obtained:

- 1) The effect of Schmidt number is to decrease the velocity distribution and concentration distribution of the fluid across the channel.
- 2) As frequency of oscillation increases; velocity, temperature and concentration decreases
- 3) Increase in radiation increases the rate of heat transfer at upper wall and decreases it at lower wall.
- 4) Increase in Peclet number decreases the rate of heat transfer at upper wall and increases it at lower wall.

- 5) As frequency of oscillation increases; rate of heat transfer at both upper and lower wall increases, rate of mass transfer at lower wall increases but rate of mass transfer at upper wall decreases.
- 6) Schmidt number decreases the rate of mass transfer at upper wall and increases it at lower wall.

REFERENCES

1. FALADE, J.A., UKAEGBU, J.C., EGERE, A.C. & ADESANYA, S.O. (2017). MHD Oscillatory flow through a porous channel saturated with porous medium. *Alexandria Engineering Journal*, **56**(1): 147-152.
2. NANDI, S. & KUMBHAKAR, B. (2021). Hall current and thermo-diffusion effects on magnetohydrodynamics convective flow near an oscillatory plate with vamped type thermal and solutal boundary conditions. *India Journal of Physics*, **Doi: 10.1007/S12648-020-02001-0**.
3. OLAJUWON, B.I. & OAHIMIRE, J.I. (2014). Effect of heat source and thermal-diffusion on MHD heat and mass transfer flow of a micropolar fluid over a vertical permeable plate. *Journal of Nigerian Association of Mathematical Physics*, **28**(1): 261-274.
4. ALI, A. & ASGHAR, S. (2014). Analytical solution for oscillatory flow in a channel for Jeffrey fluid. *Journal of Aerospace Engineering*, **27**(3): 644-651
5. MASUDA, T. & TAGAWA, T. (2019). Quasi-periodic oscillating flows in a channel with suddenly expanded section. *Journal of Symmetry in Fluid*, **11**(11): 1403-1418
6. TABAKOVA, S., KUTEV, N. & RADEV, S.T. (20220). Oscillatory carreau flows in straight channels. *Royal Society Open Science*, <https://doi.org/10.1098/rso5.191305>.
7. KALPANA, M. & VIJAYA, R.B. (2019). Hall effects on MHD oscillatory flow of non-Newtonian fluid through porous medium in a vertical channel with suction/injection. *International journal of Applied Engineering Research*, **14**(21): 3960-3967.
8. HACIOGLU, A. & NARAYANAN, R. (2016). Oscillating flow and separation of species in rectangular channels. *Physics of Fluids*, **28**: 073603
9. SALEEM, M., TUFAIL, N. & ALI, O. (2020). An oscillation effects on MHD radiative casson fluid flows in an asymmetric channel through group theoretical analysis. *Canadian Journal of Physics*, **98**(1): 81-88.
10. SHARMA, A. & DUBEWAR, A.V. (2019). MHD flow between two parallel plates under the influence of inclined magnetic field by finite difference method. *International Journal of Innovative Technology and Exploring Engineering*, **8**(12): Page
11. MAKINDE, O.D. & MBONE, P.Y. (2005). Heat transfer to MHD oscillatory flow in a channel filled with porous medium. *Romanian Journal of Physics*, <https://www.researchgate.net/publication/228762638>.
12. CHOUDHURRY, R. & DAS, U.J. (2012). Heat transfer to MHD oscillatory viscoelastic flow in a channel filled with porous medium. *International Journal of Physics Research*, **Doi:10.1155/2012/879537**.
13. COGLEY, A.C., VINCENT, W.G. & GILES, E.S. (1968). Differential approximation for radiative heat transfer in non-linear equations-grey gas near equilibrium. *American Institute of Aeronautics and Astronautics*, **6**: 551-553.
14. NIRMALA, P.R., BALAKRISHNAN, V. & VASANTHAKUMARI, R. (2018). MHD Transport Phenomena of Oscillatory channel of blood flow with Hall current. *International Journal of Mathematic Trends and Technology*, **54**(2): 164-175.

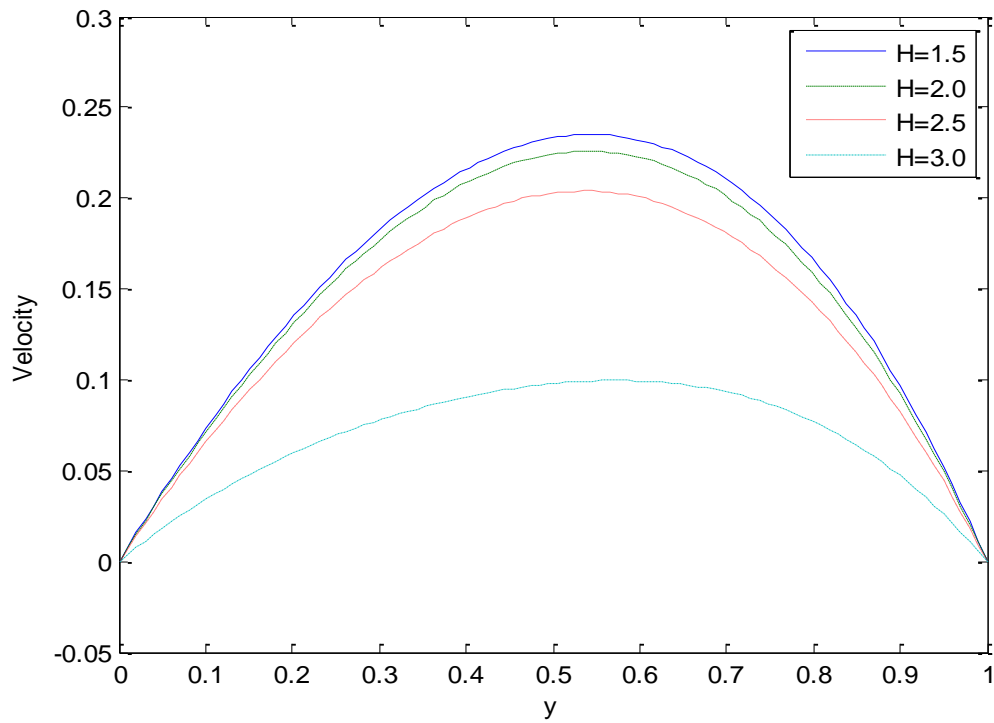


Figure 2: Velocity profiles for different values of Hartmann number.

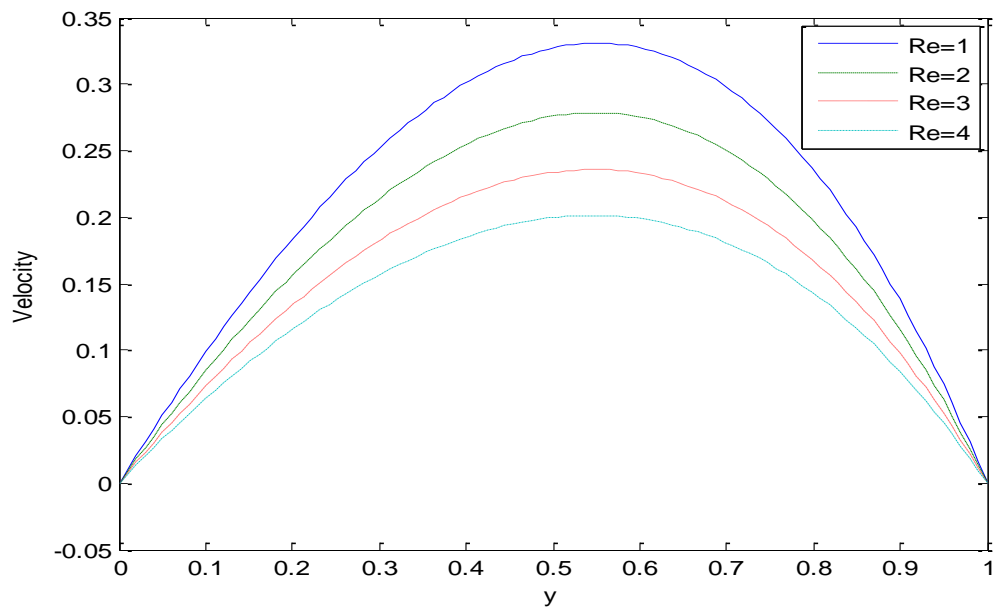


Figure 3: Velocity profiles for different values of Reynolds number.

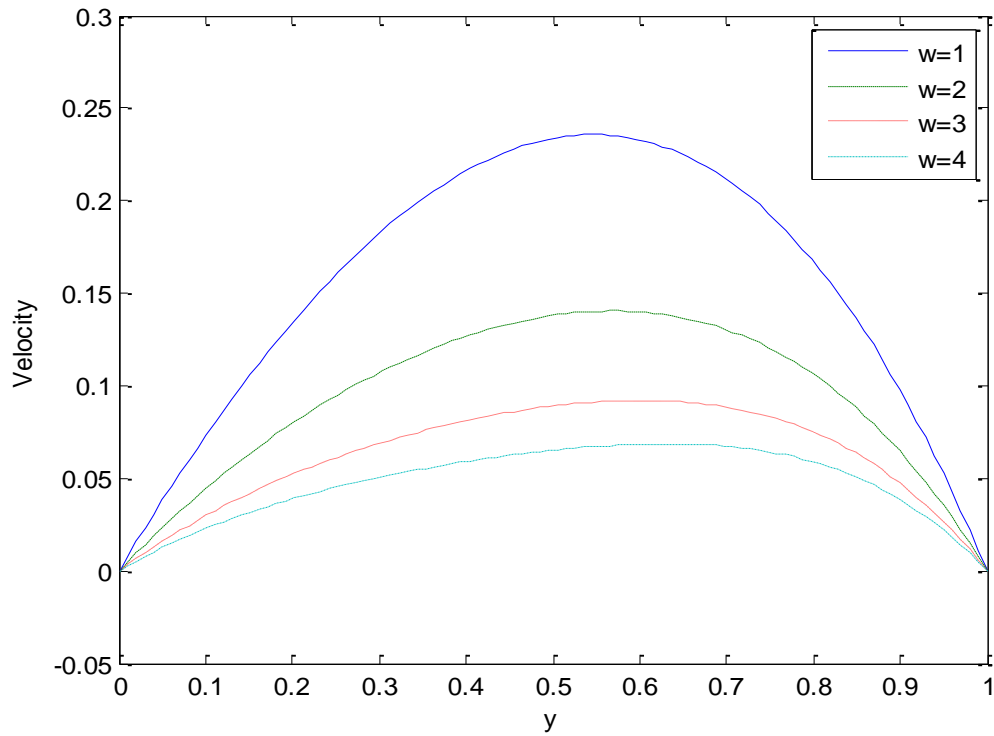


Figure 4: Velocity profiles for different values of frequency of oscillation parameter.

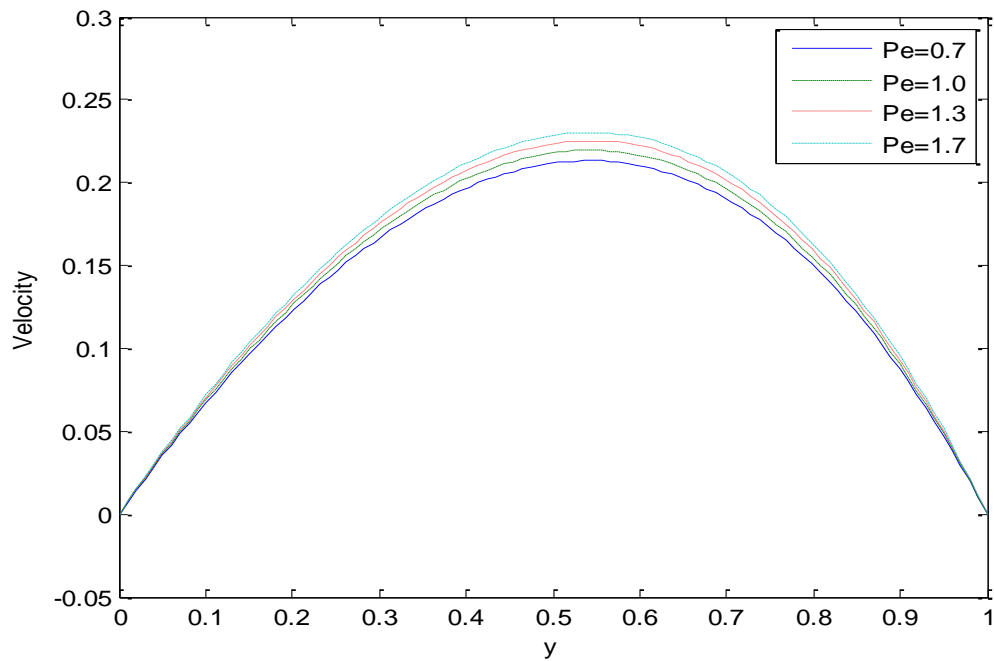


Figure 5: Velocity profiles for different values of Peclet number.

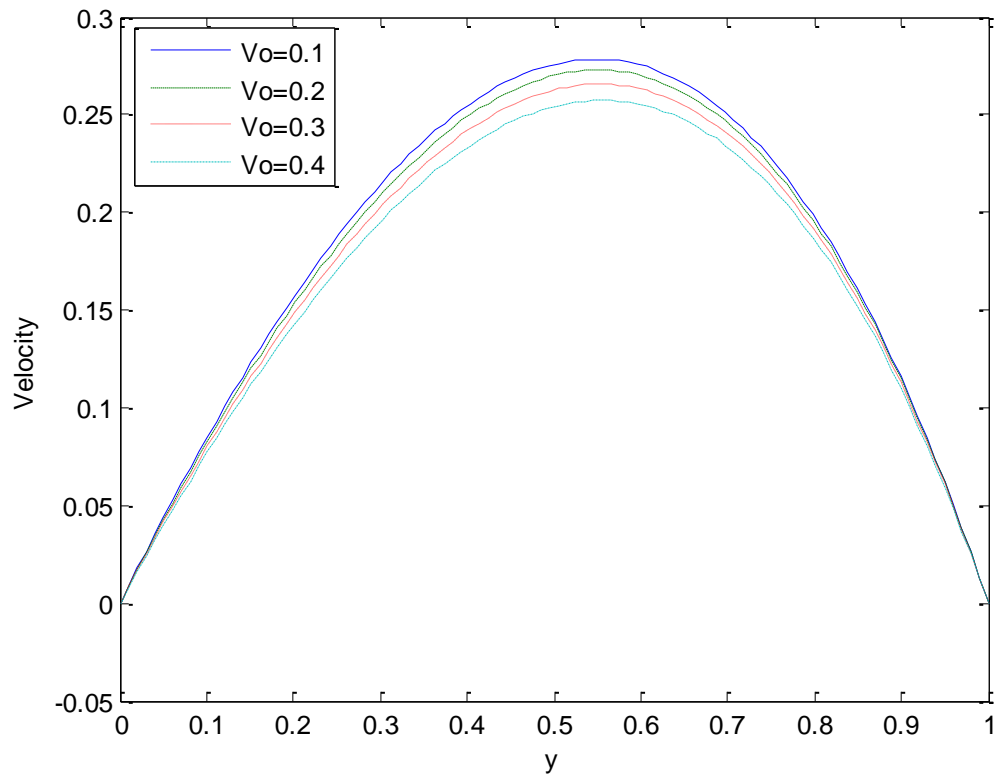


Figure 6: Velocity profiles for different values of viscoelastic parameter.

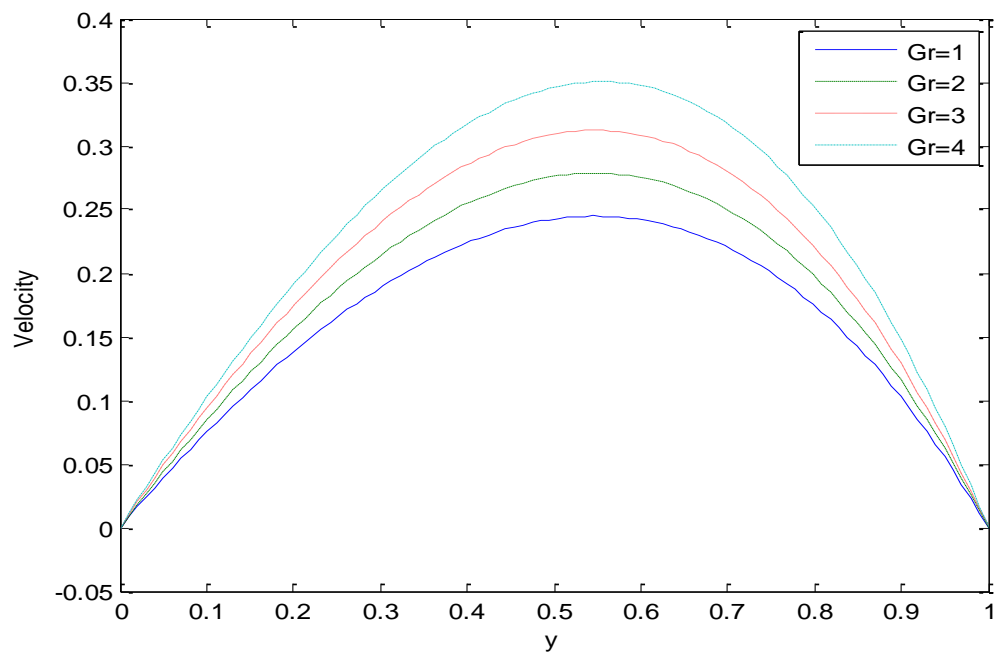


Figure 7: Velocity profiles for different values of Grashof number.

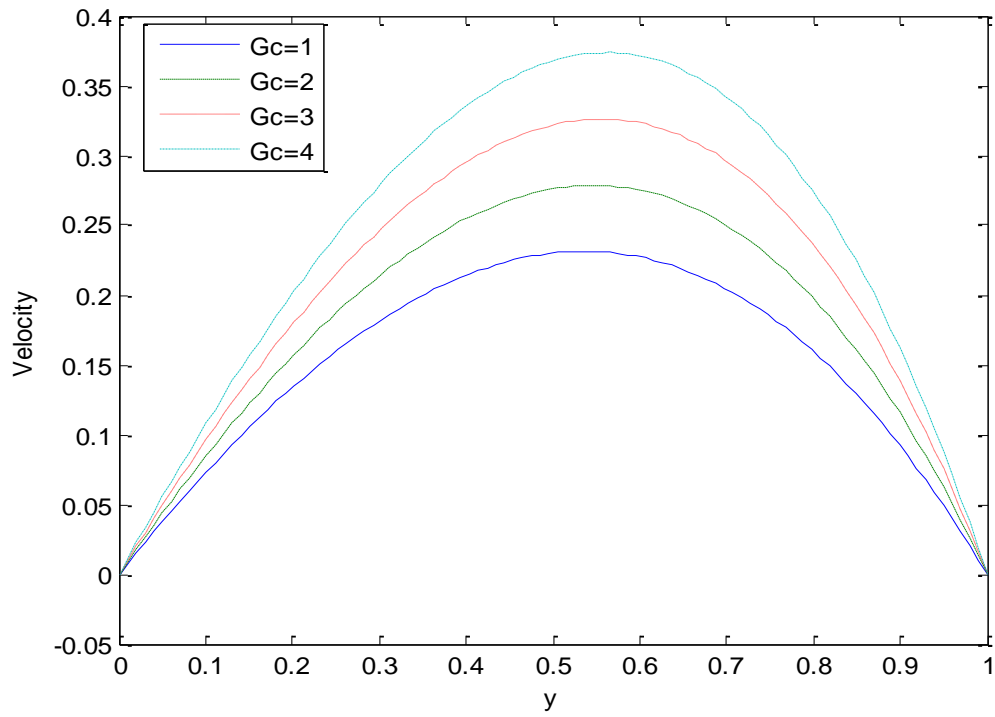


Figure 8: Velocity profiles for different values of modified Grashof number.

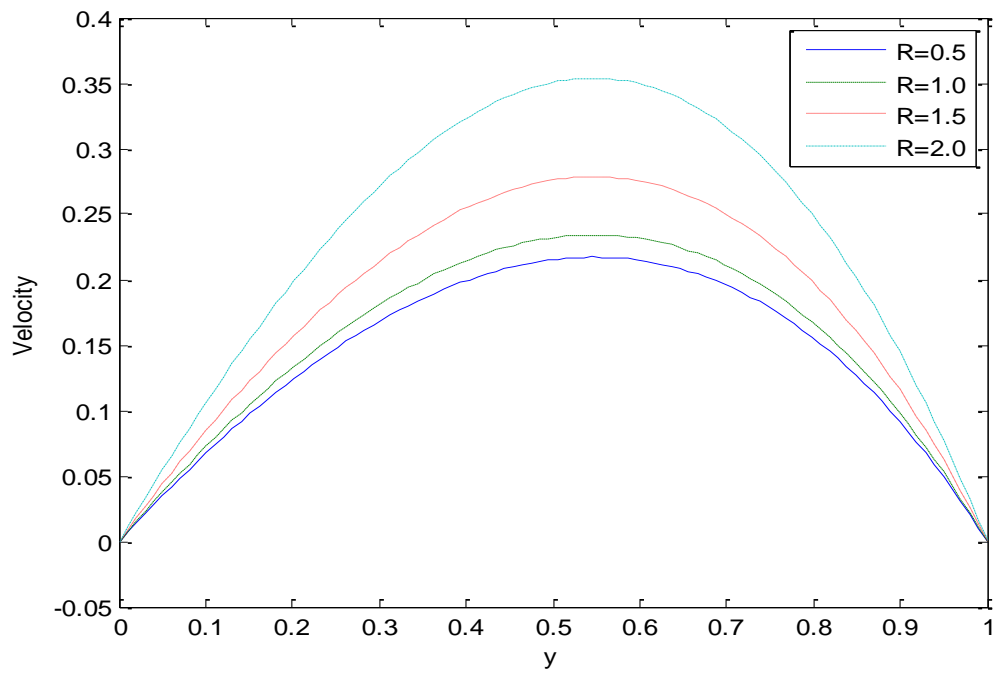


Figure 9: Velocity profiles for different values of radiation parameter.

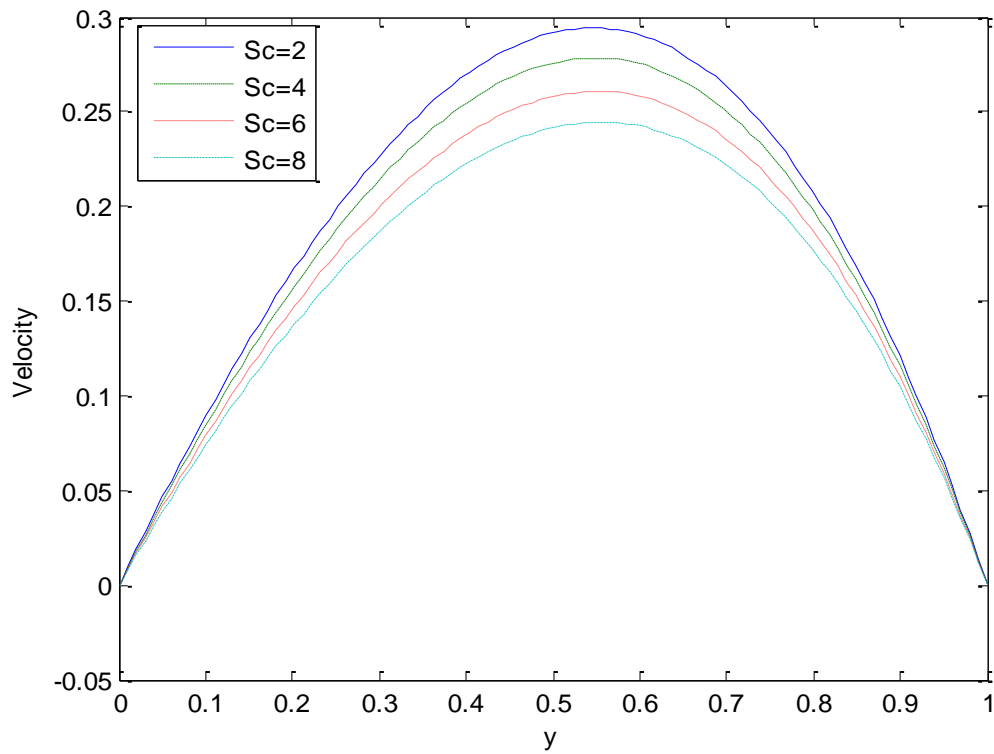


Figure 10: Velocity profiles for different values of Schmidt number.

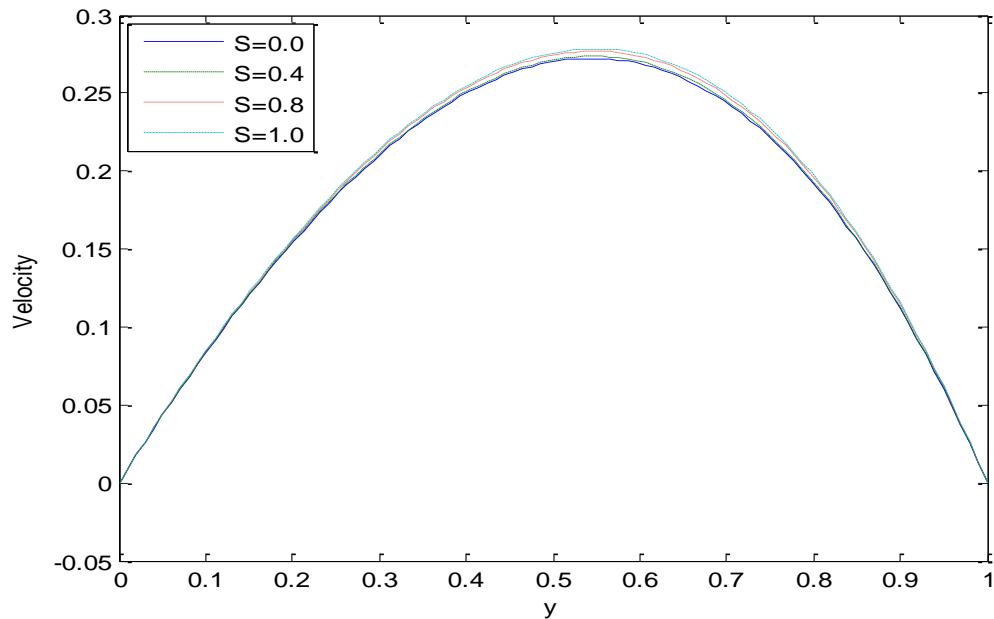


Figure 11: Velocity profiles for different values of porous medium shape parameter

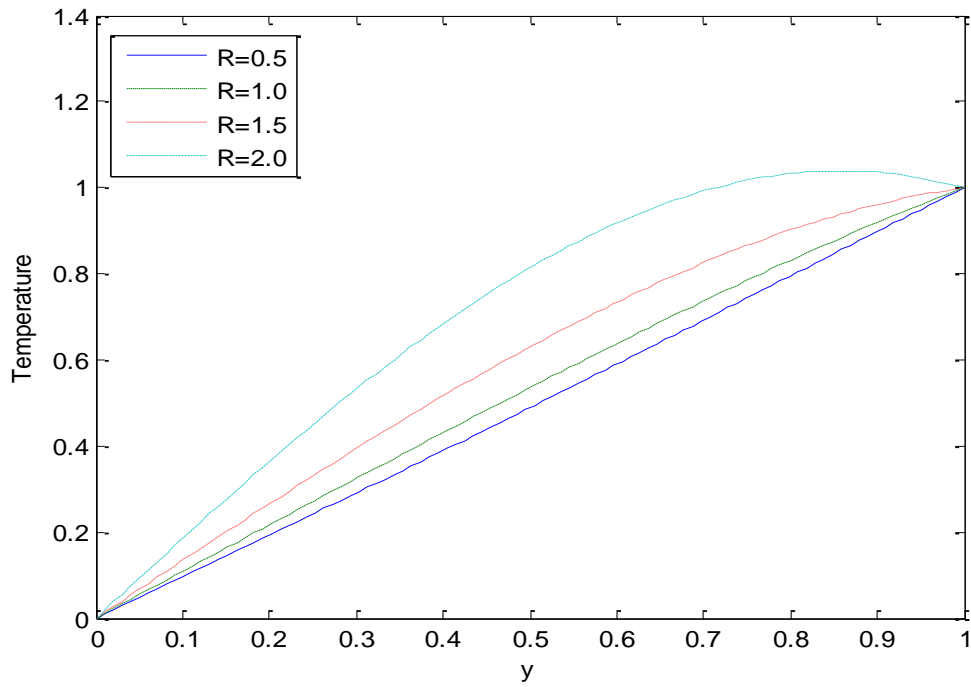


Figure 12: Temperature profiles for different values of radiation parameter

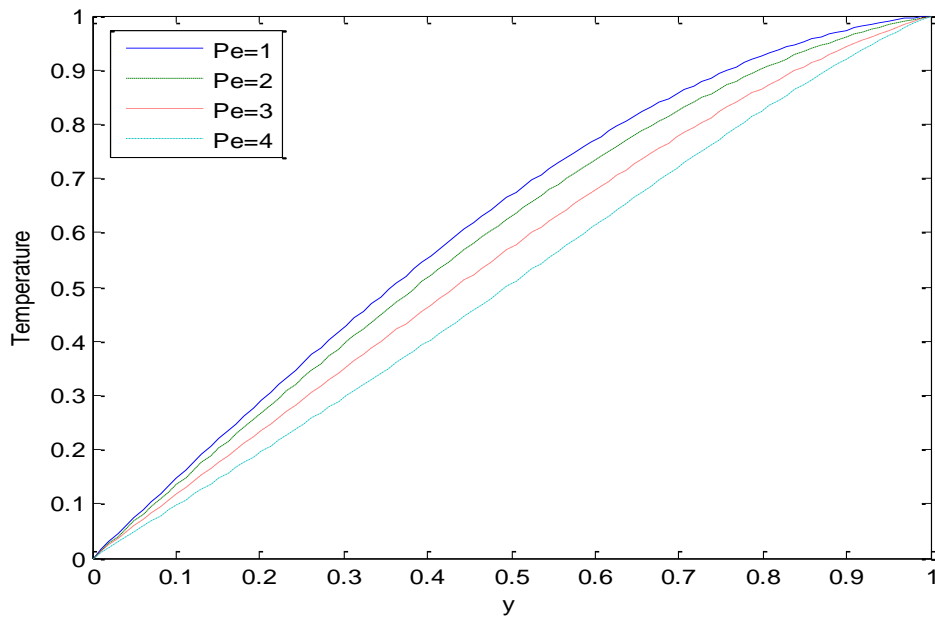


Figure 13: Temperature profiles for different values of Peclet number

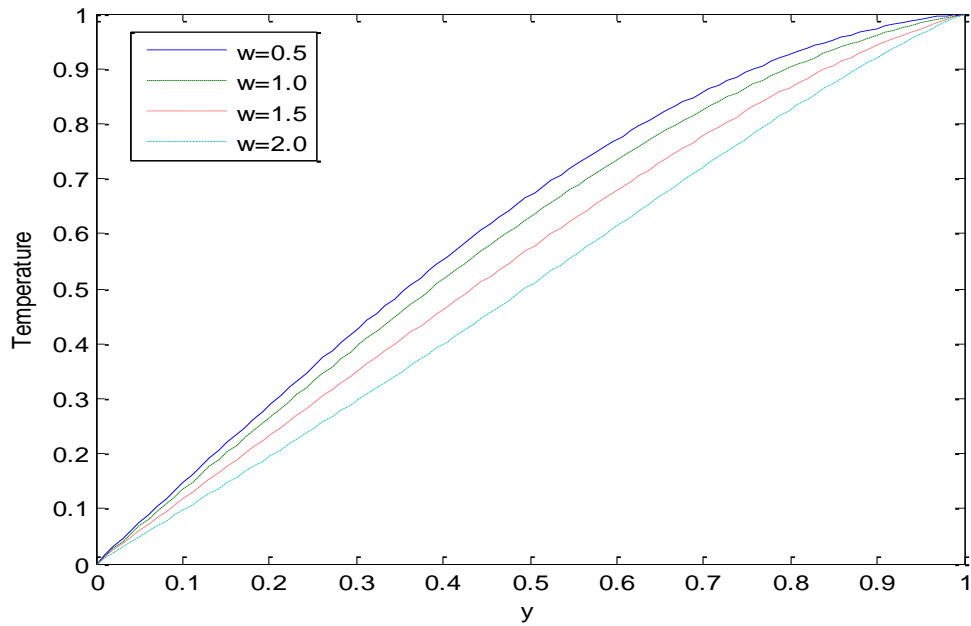


Figure 14: Temperature profiles for different values of oscillation parameter

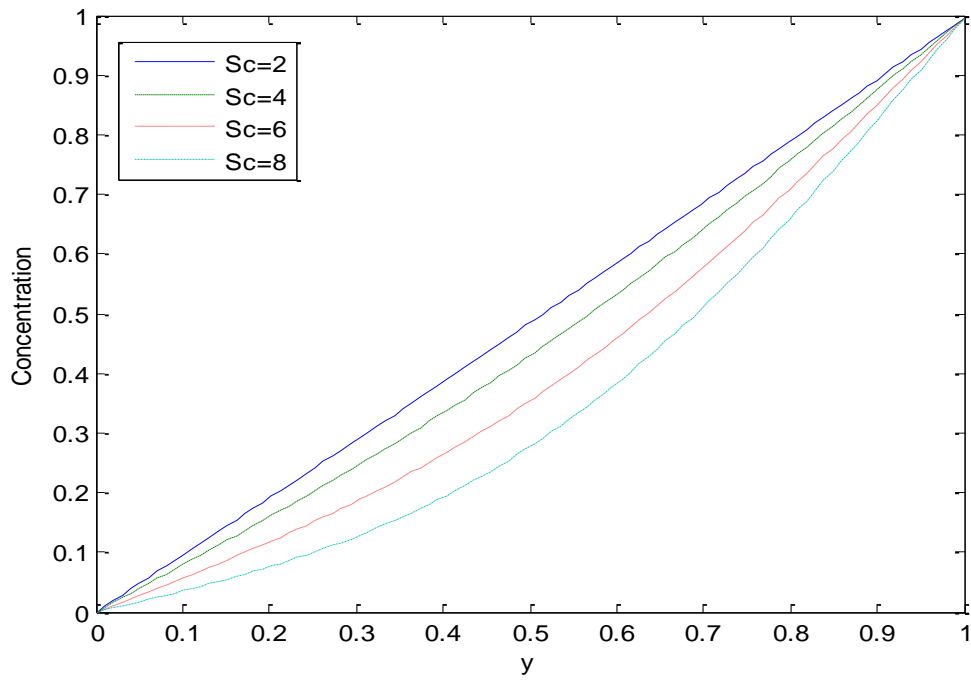


Figure 15: Concentration profiles for different values of Schmidt number.

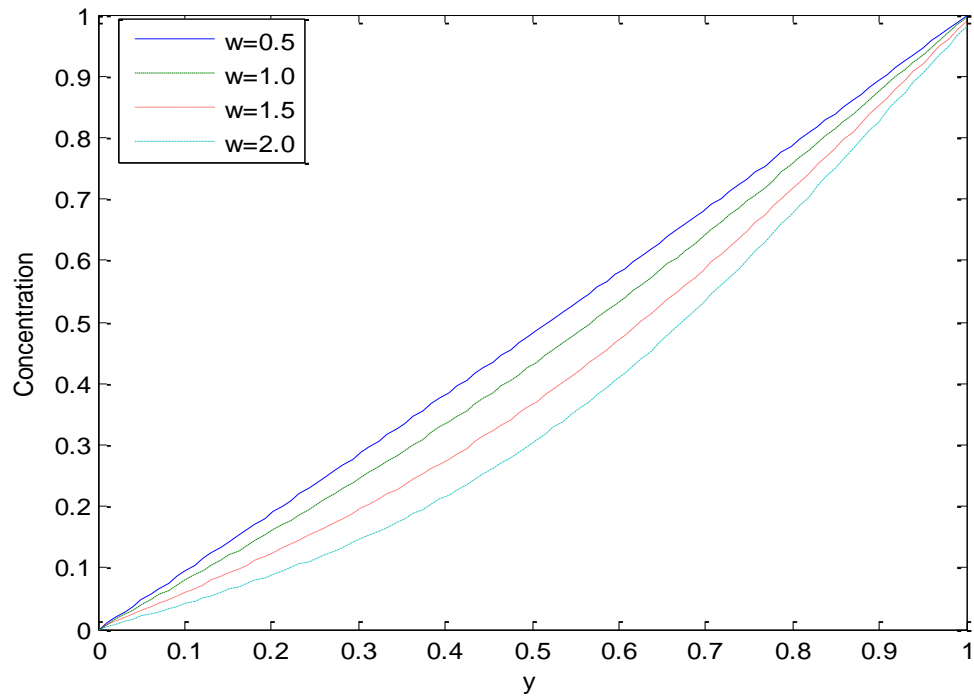


Figure 16: Concentration profiles for different values of oscillation parameter.